ACS APPLIED MATERIALS & INTERFACES

Research Article

www.acsami.org

Structural and Electronic Properties of Silicene on MgX_2 (X = Cl, Br, and I)

Jiajie Zhu and Udo Schwingenschlögl*

PSE Division, King Abdullah University of Science and Technology, Thuwal 23955-6900, Kingdom of Saudi Arabia

ABSTRACT: Silicene is a monolayer of Si atoms in a two-dimensional honeycomb lattice, being expected to be compatible with current Si-based nanoelectronics. The behavior of silicene is strongly influenced by the substrate. In this context, its structural and electronic properties on MgX_2 (X = Cl, Br, and I) have been investigated using first-principles calculations. Different locations of the Si atoms are found to be energetically degenerate because of the weak van der Waals interaction with the substrates. The Si buckling height is below 0.55 Å, which is close to the value of free-standing silicene (0.49 Å). Importantly, the Dirac cone of silicene is well preserved on MgX_2 (located slightly above the Fermi level), and the band gaps induced by the substrate are less than 0.1 eV. Application of an external electric field and stacking can be used to increase the band gap.

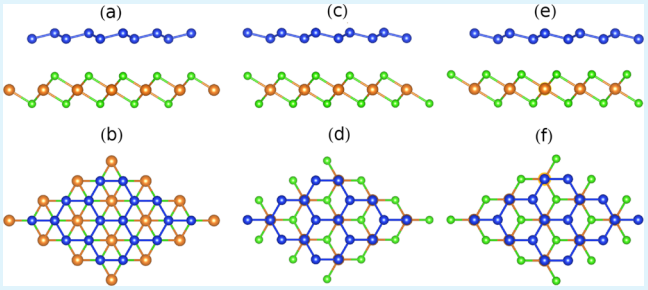

KEYWORDS: *silicene, substrate, strain, electric field*

1. INTRODUCTION

Graphene is probably the most famous two-dimensional material because of its unusual electronic properties, resulting from the planar honeycomb structure and an extensive range of possible applications in nanoelectronics.[1−3] Because of the novel applications opened by graphene, increasing efforts have been dedicated to the search for other two-dimensional group IV materials, especially to Si. Silicene, a monolayer of Si atoms in a honeycomb structure, was first addressed theoretically by Takeda and Shiraishi in 1994.[4] Free-standing silicene, unlike graphene, is predicted to be subject to a slight buckling due to sp^2−sp^3 hybridization. The linearly dispersing π and π^* bands crossing the Fermi level at the K point of the Brillouin zone resemble the massless Dirac Fermions of graphene.[5] Strong spin−orbit coupling makes silicene to a promising candidate for hosting quantum-spin Hall physics.[6] Furthermore, silicene is expected to be better compatible with the current Si-based technology than graphene.

Although free-standing silicene probably cannot exist in nature, the material has been successfully deposited on metallic substrates such as ZrB_2(0001), Ir(111), and Ag(111).[7−11] The latter has attracted much attention because of the low lattice mismatch of 0.3%. However, the π bands of silicene are subject to strong hybridization with Ag, destroying the Dirac cone.[12,13] On the other hand, several semiconductors have been explored theoretically to overcome the strong interaction characteristic for metallic substrates. For example, Ding and Wang have reported that GaS nanosheets could preserve the linearly dispersing bands with a gap of 0.17 eV, but the lattice mismatch would amount to 7.5%.[14] Although the lattice mismatch is smaller (2.3%) for ZnS(0001), this substrate also perturbs the band structure.[15] Bhattacharya and co-workers have investigated II−VII and III−VI semiconductor substrates such as AlAs(111) and ZnSe(111).[16] They report that the stability and electronic properties of these systems depend largely on the topmost atoms of the substrate.

Perturbations of the band structure of silicene are related to dangling bonds of the substrate.[17,18] Accordingly, preservation of the Dirac cone has been achieved by H passivation of these bonds both for Si- and C-terminated SiC(0001).[19] F-terminated CaF_2(111) is also predicted to preserve the Dirac cone with a gap of 52 meV.[20] However, there are two F layers and one Ca layer along the [111] direction, and only one of the F-terminated (111) planes has no dangling bond, which requires accurate control during preparation of the material. In addition, the multilayer technique may be helpful to screen the interaction between silicene and the substrate, as has been demonstrated for graphene.[21,22] However, strong interlayer interaction can perturb the π bands.[23] Intercalation of F and/or H could possibly help to solve this problem.[24] Not only will the electronic properties of silicene be less affected by a substrate without dangling bonds, but also the preparation procedure will be simplified. The compounds MgX_2 (X = Cl, Br, and I) are insulators with hexagonal structures and form layers along the [0001] direction without dangling bonds. $MgCl_2$ has been synthesized on different substrates.[25,26] Being therefore interesting candidates for substrates and having not received attention so far, the structural and electronic properties of silicene on MgX_2(0001) will be investigated in this paper using first-principles calculations.

Received: April 23, 2014
Accepted: June 24, 2014
Published: July 8, 2014

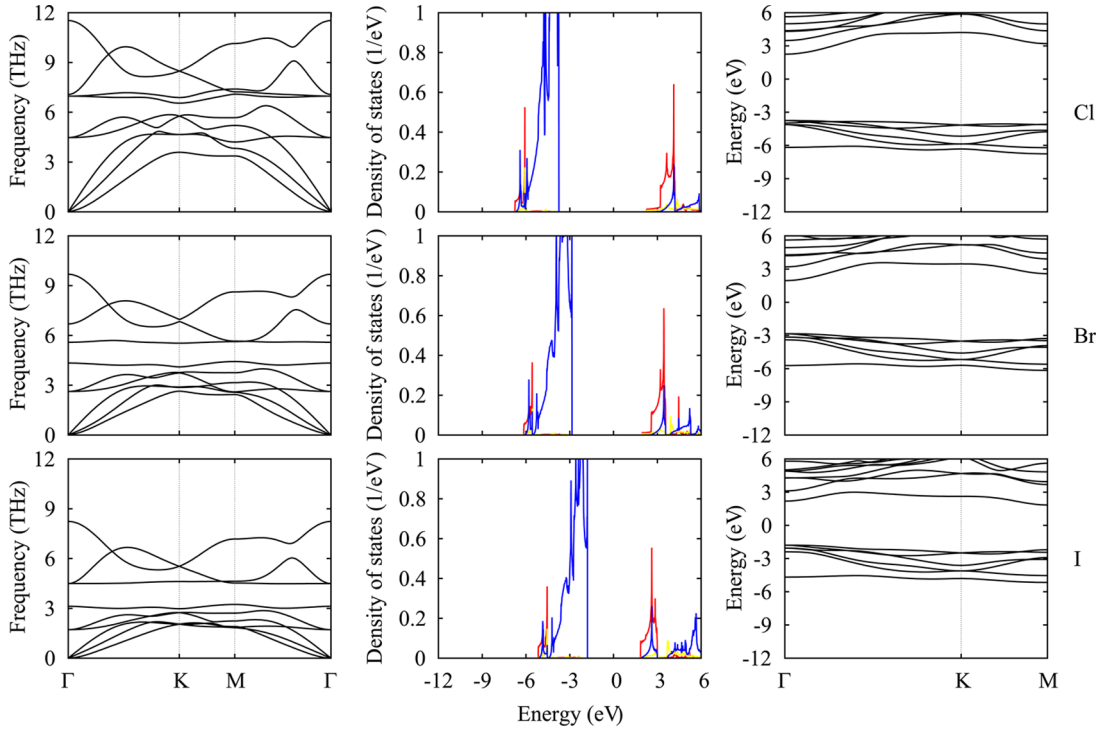

Figure 1. Phonon dispersion (left), density of states (middle), and band structure (right) of monolayer $MgX_2(0001)$ (X = Cl, Br, and I). The Mg 3s, X s, and X p states are shown in red, yellow, and blue.

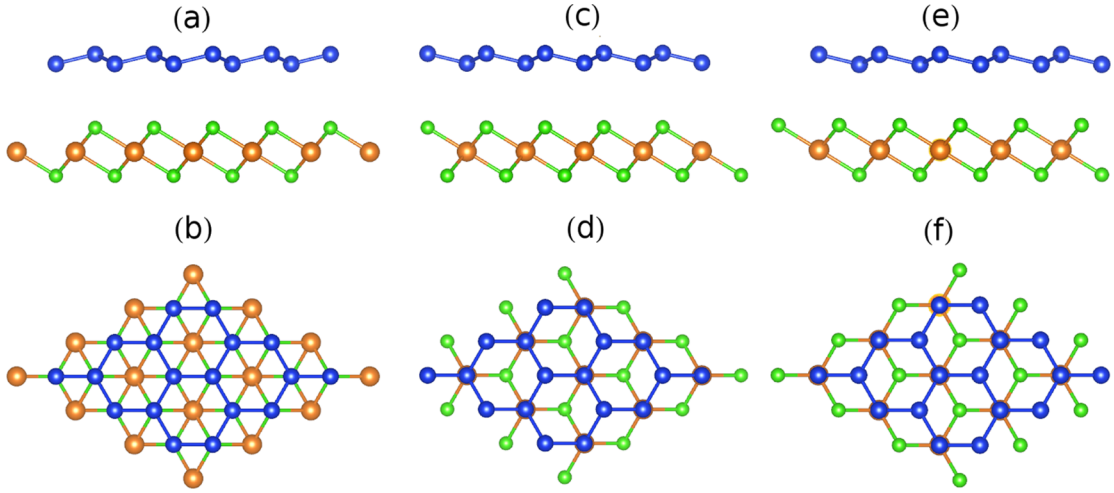

Figure 2. (a, c, and e) Top and (b, d, and f) side views of silicene on $MgBr_2(0001)$ for configurations A–C, respectively. Mg, Br, and Si atoms are shown in brown, green, and blue.

2. COMPUTATIONAL METHOD

Calculations are performed within the framework of density functional theory (DFT) using the projector-augmented plane-wave method, as implemented in the Vienna Ab-initio Simulation Package.[27,28] The generalized gradient approximation of Perdew, Burke, and Ernzerhof is selected for the exchange-correlation potential,[29] and the DFT-D2 method is employed to consider long-range van der Waals interactions.[30] Brillouin zone integrations are carried out with 15 × 15 × 1 *k* meshes for the structure optimizations and 36 × 36 × 1 *k* meshes for the band structure calculations. The cutoff energy for the plane-wave basis is set to 500 eV in order to achieve an energy accuracy of 1 meV. Moreover, we use an energy tolerance of 10^{-8} eV in the iterative solution of the Kohn–Sham equations, and the structures are relaxed until the residual forces on the atoms have declined to less than 0.01 eV/Å. The phonon calculations are based on the Parlinski–Li–Kawazoe method, as implemented in *Phonopy*.[31,32]

The substrate is modeled by a 1 × 1 MgX_2 monolayer with a vacuum slab of 15 Å thickness on top to avoid unphysical interactions between periodic images. We also consider sandwich structures in which $MgBr_2$ is attached to both sides of the silicene sheet. The electronic bands of $MgCl_2$ and MgI_2 are found to be only slightly distorted in spite of large lattice mismatches. A trilayer slab is studied for $MgBr_2$ to compare with the monolayer results.

3. RESULTS AND DISCUSSION

The calculated in-plane lattice constants of monolayer $MgX_2(0001)$ (X = Cl, Br, and I) are 3.621, 3.830, and 4.150 Å for X = Cl, Br, and I, respectively, and the corresponding experimental values are 3.641, 3.815, and 4.154 Å.[33−35]

Table 1. Structural Properties of Silicene on $MgX_2(0001)$ (X = Cl, Br, and I) for Configurations A–C, Including the Si Buckling Height (b_{Si}), Bond Length between Si Atoms (d_{Si}), Distance between Silicene and the Substrate (d_{Si-sub}), In-Plane Lattice Constant (a), and Binding Energy per Si Atom (E)

	configuration		
	A	B	C
	$MgCl_2$		
b_{Si} (Å)	0.55	0.55	0.55
d_{Si} (Å)	2.25	2.25	2.25
d_{Si-sub} (Å)	3.56	3.64	3.28
a (Å)	3.770	3.772	3.773
E (meV/Si)	34	33	46
	$MgBr_2$		
b_{Si} (Å)	0.49	0.49	0.49
d_{Si} (Å)	2.27	2.27	2.27
d_{Si-sub} (Å)	3.58	3.58	3.23
a (Å)	3.836	3.835	3.837
E (meV/Si)	45	44	63
	MgI_2		
b_{Si} (Å)	0.39	0.40	0.39
d_{Si} (Å)	2.32	2.32	2.32
d_{Si-sub} (Å)	3.73	3.75	3.28
a (Å)	3.962	3.960	3.960
E (meV/Si)	56	53	88

Moreover, the lattice constant of free-standing silicene is 3.848 Å. The Mg–X bond length amounts to 2.52, 2.69, and 2.95 Å for X = Cl, Br, and I because of the increasing atomic radius of X. The phonon dispersion relation, density of states, and band structure of monolayer $MgX_2(0001)$ are addressed in Figure 1. The phonon spectra show no imaginary frequencies, predicting the stability of the substrates. Decreasing frequencies from $MgCl_2$ to MgI_2 are due to the increasing mass of the halide atoms. The top of the valence band is dominated by the X p states, while the bottom of the conduction band mainly consists of the Mg 3s states. The band gap is 6.0, 4.8, and 3.6 eV for $MgCl_2$, $MgBr_2$, and MgI_2, respectively, because of the decreasing electronegativity of the halide atoms.

Figure 2 shows silicene on $MgBr_2(0001)$ for different locations of the Si atoms, namely, on top of Mg, Br, and the hollow site. In configuration A, the Si atoms are located on top of Br and the hollow site, in configuration B, on top of Mg and Br, and in configuration C, on top of Mg and the hollow site. The same configurations are considered for $MgCl_2$ and MgI_2. Configuration C turns out to be the most stable for all of the substrates. However, the configurations are energetically almost degenerate with maximal differences of 5, 8, and 14 meV per atom for $MgCl_2$, $MgBr_2$, and MgI_2, respectively, because of a lack of unsaturated bonds on the substrate.

The structural properties of silicene on the different substrates are listed in Table 1. On $MgBr_2$, the lattice constant is found to be about 3.837 Å, thus slightly shorter than the corresponding value of free-standing silicene (3.848 Å). Although the lattice constant is the same as that for silicene on Ag(111), the buckling height of the Si atoms is much smaller (0.49 Å instead of 0.75 Å) and therefore close to the value of free-standing silicene (0.47 Å).[9] The distance between silicene and the $MgBr_2$ substrate in configuration C amounts to 3.23 Å, which is substantially larger than that in the case of an Ag(111) substrate (2.44 Å).[12] Furthermore, a small binding energy below 63 meV per Si atom reflects weak van der Waals interactions between silicene and the substrate. Note that the total energy per Si atom in diamond is about 0.5 eV lower than that in two-dimensional silicene. Two Si layers on top of the substrate thus will form clusters instead of a silicene bilayer, suggesting the importance of avoiding multilayers in the preparation of silicene. A trilayer slab of $MgBr_2$ yields little variation for the structural properties of silicene in configuration C. The in-plane lattice constant is 3.834 Å, which is 0.1% smaller than the monolayer result. The Si buckling height (0.49 Å) and distance between silicene and the substrate (3.26 Å) are also close to the corresponding monolayer values. Moreover, the binding energy of 63 meV per Si atom equals that of the monolayer. Therefore, the monolayer model is appropriate to describe the structural properties.

Variation of the lattice constant of silicene on $MgCl_2$ and MgI_2 amounts to −1.9% and +2.9%, respectively, compared to the free-standing case. This leads to changes in the Si bond length and buckling height. Enforcing the lattice constant of free-standing silicene for configuration C results in a 0.18 Å increase and a 0.04 Å decrease of the distance between silicene and the substrate for $MgCl_2$ and MgI_2, respectively, and a corresponding 3 meV decrease and 7 meV increase in the binding energy. Configurations A and B show lower binding energies and larger distances to the different substrates due to modifications in the charge distribution.

Figure 3 illustrates the charge density difference

$$\Delta\rho = \rho_t - \rho_{sub} - \rho_{Si}$$

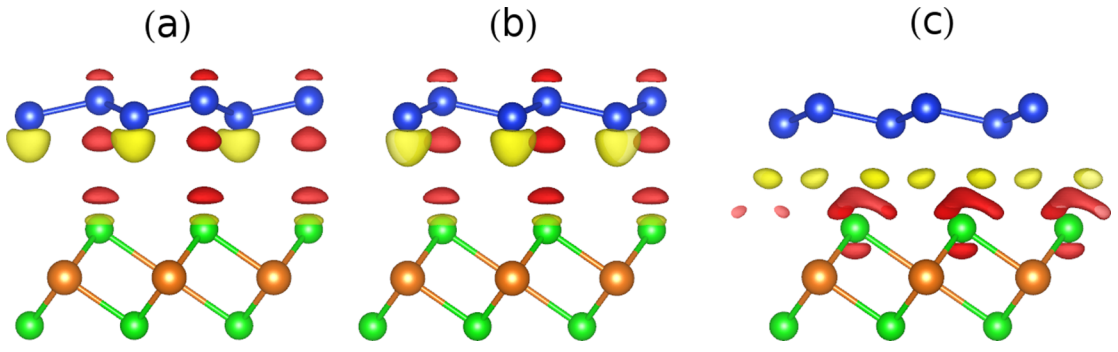

Figure 3. Charge density difference for silicene on $MgBr_2(0001)$ for configurations (a) A, (b) B, and (c) C. Yellow/red represents charge accumulation/depletion, where the isosurfaces refer to isovalues of 1.6×10^{-4} electrons/bohr^3. Mg, Br, and Si atoms are shown in brown, green, and blue.

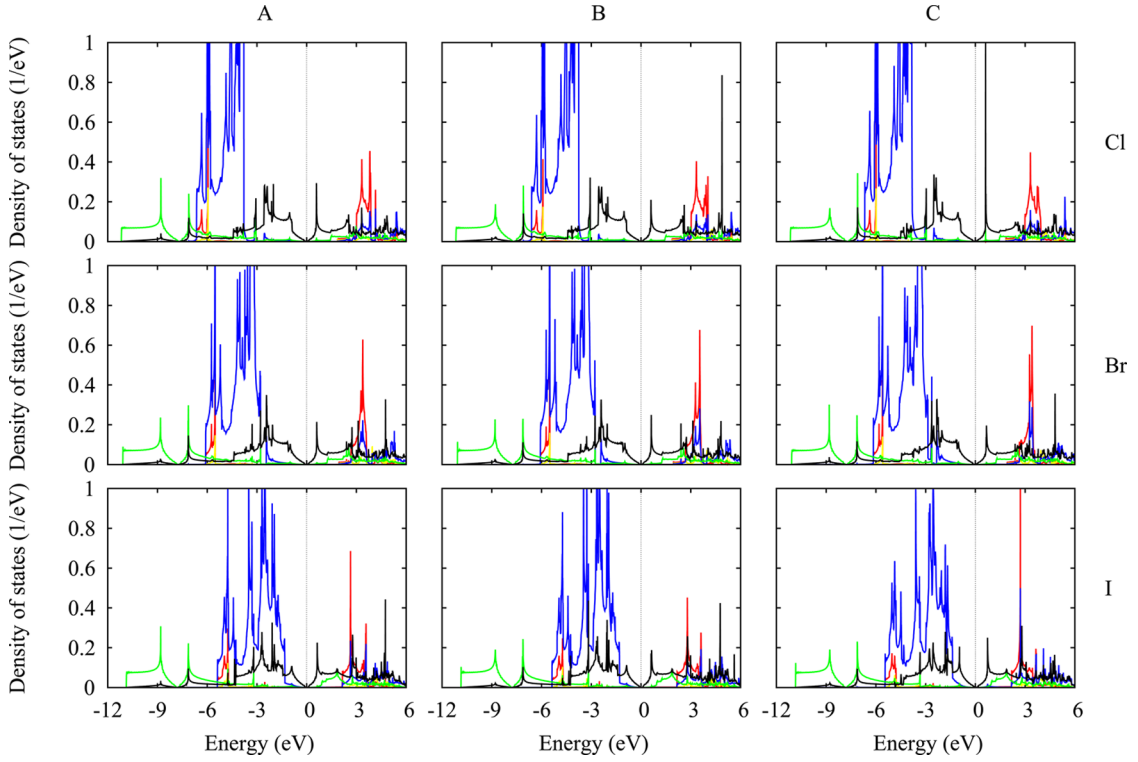

Figure 4. Density of states of silicene on $MgX_2(0001)$ (X = Cl, Br, and I) for configurations A−C. The Fermi level is set to zero. The Mg 3s, X s, X p, Si 3s, and Si 3p states are shown in red, yellow, blue, green, and black.

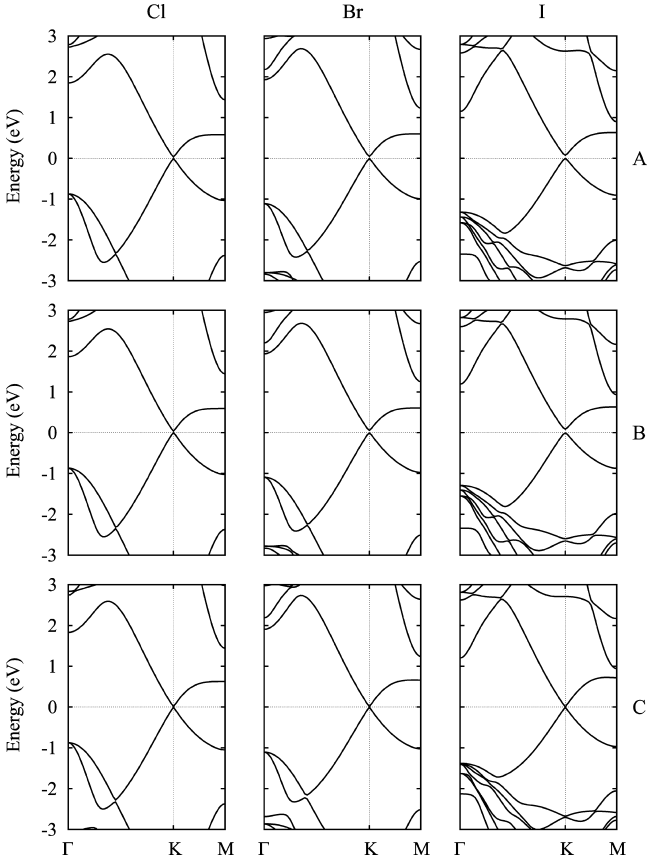

Figure 5. Band structure of silicene on $MgX_2(0001)$ (X = Cl, Br, and I) for configurations A−C. The Fermi level is set to zero.

Table 2. Position of the Dirac Point above the Fermi Energy (E_D) and Gap at the Dirac Point (E_g)[a]

	configuration		
	A	B	C
	$MgBr_2$		
E_D (meV)	13	19	2 (4)
E_g (meV)	41	40	16 (9)
	$MgBr_2$		
E_D (meV)	18	24	2
E_g (meV)	53	64	13
	MgI_2		
E_D (meV)	36	39	0 (2)
E_g (meV)	73	90	1 (10)

[a]The values in parentheses are calculated using the lattice constant of free-standing silicene.

of silicene on $MgBr_2(0001)$ for the different configurations, where ρ_t, ρ_{sub}, and ρ_{Si} are the charge densities of the full system, substrate, and silicene sheet, respectively. The latter two values are calculated with the atoms at the same positions as those in the full system. The charge density difference highlights the redistribution of charge due to interaction at the interface. Charge transfer in configurations A and B mainly occurs within the silicene sheet from the upper Si atom to the lower Si atom. In the case of configuration C, a strong charge transfer is found in the interstitial region between these two subsystems because of the different locations of the Si atoms. Note that the Si atoms on top of the hollow sites of the Br layer here have higher symmetry than those in configurations A and B. The charge transfer from the silicene sheet to the substrate calculated by the Bader approach is below 0.015 electrons because of the weak van der Waals interaction between the two subsystems.

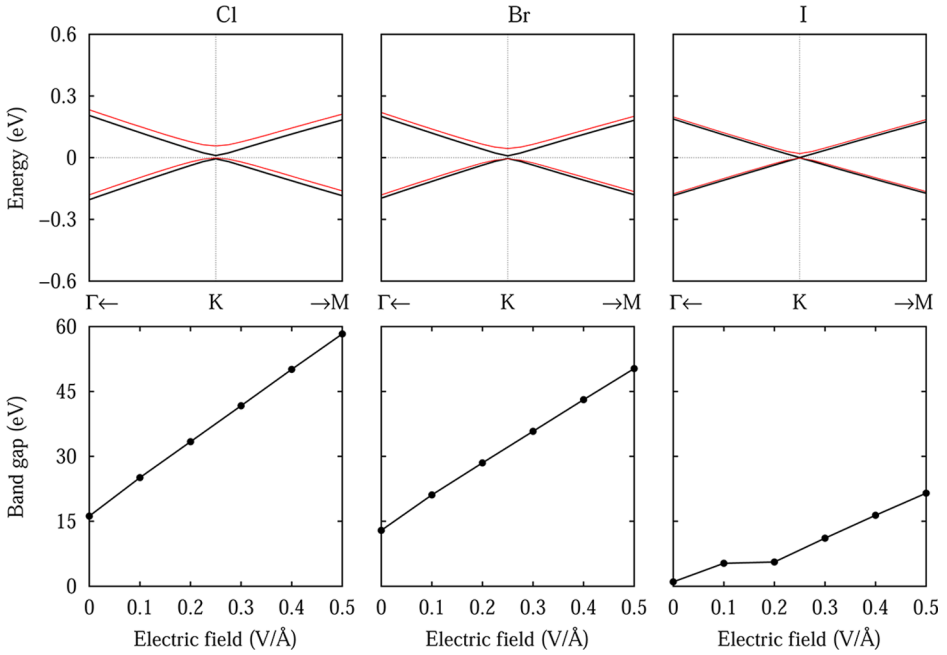

Figure 6. Band structure of silicene on $MgX_2(0001)$ (X = Cl, Br, and I) in configuration C for an external perpendicular electric field of 0 (black) and 0.5 V/Å (red) with the Fermi level at zero as well as field dependence of the band gap.

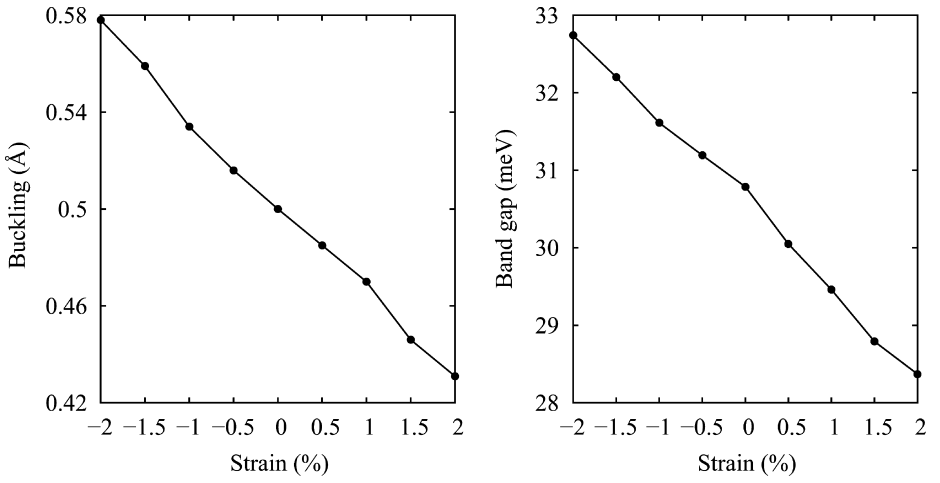

Figure 7. Strain dependence of the buckling and band gap for the $MgBr_2(0001)$−silicene−$MgBr_2(0001)$ sandwich (configuration CC).

The density of states of silicene on $MgX_2(0001)$ (X = Cl, Br, and I) is shown in Figure 4 for different configurations. The top of the valence band and bottom of the conduction band are dominated by Si 3p states. The gap between the X p and Mg 3s states decreases from $MgCl_2$ to MgI_2, which is similar to the pure substrates, and the distance from the X p states to the top of the valence band decreases. Furthermore, the increasing hybridizaion between the X p and Si 3p states reflects a growing interaction between silicene and the substrate.

Figure 5 shows the band structure of silicene on $MgX_2(0001)$ (X = Cl, Br, and I) for the different configurations. The linearly dispersing π band of free-standing silicene is well preserved in each case. The Dirac point is located slightly above the Fermi level, reflecting very weak p doping, where the K and K′ points of the Brillouin zone are equilvalent. The Fermi velocity of free-standing silicene is found to be 5.56×10^5 m/s, in good agreement with previous theoretical values.[36] The corresponding values are 5.35×10^5, 5.29×10^5, and 5.09×10^5 m/s for silicene on $MgCl_2$, $MgBr_2$, and MgI_2 in configuration C, respectively, because of the increasing interaction.

The band gap of free-standing silicene is 0.1 meV, with the Dirac point located at the Fermi level. For the hybrid systems, Table 2 lists the location of the Dirac point with respect to the Fermi level and respective band gap. The latter is much larger for configurations A and B than for configuration C because of the larger charge transfer within the two sublattices of silicene; see Figure 3. Moreover, the band gap increases from $MgCl_2$ to MgI_2 with an upward shift of the Dirac point for configurations A and B (increasing interaction). Because the band gap is also influenced by variation of the buckling induced by the lattice mismatch (as reported for free-standing silicene), we have calculated the band structure of silicene on $MgCl_2$ and MgI_2 in configuration C using the lattice constant of free-standing silicene.[36] We find band gaps of 9 and 10 meV, as listed in parentheses in Table 2. The band gap in configurations A and B is dominated by interaction with the substrate, whereas in

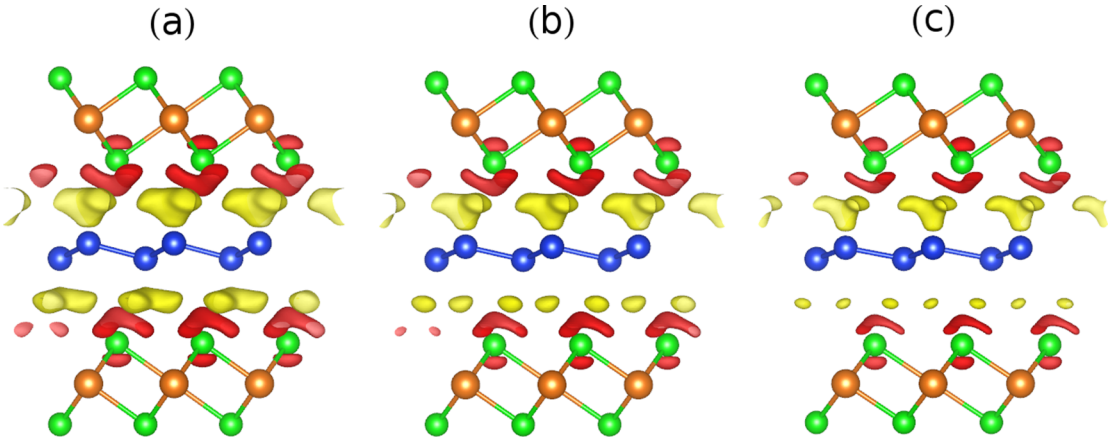

Figure 8. Charge density difference for the $MgBr_2(0001)$−silicene−$MgBr_2(0001)$ sandwich (configuration CC) under (a) −2%, (b) zero, and (c) 2% strain. Yellow/red represents charge accumulation/depletion, where the isosurfaces refer to isovalues of 1.6×10^{-4} electrons/bohr^3. Mg, Br, and Si atoms are shown in brown, green, and blue.

configuration C, this effect is much weaker (thus comparable with that of the lattice mismatch) because of the higher symmetry.

The band gaps obtained for configuration C are lower than the thermal energy at room temperature (25.8 meV), which limits applications. A perpendicular external electric field has been demonstrated to open a band gap in free-standing silicene.[37−39] Figure 6 shows the band structure of silicene on MgX_2 (X = Cl, Br, and I) in configuration C under such an electric field applied parallel to the intrinsic field between silicene and the substrate. The electric field leads to a slight distortion of the π bands, and the band gap increases with the field strength. A value of 50 meV is obtained for a field of 0.5 V/Å in the case of $MgBr_2$, which is larger than the thermal energy at room temperature. The electric field breaks the symmetry of the two silicene sublattices and induces charge transfer between them, resulting in band gap opening.[39] The effect decreases from $MgCl_2$ to MgI_2 because of the growing interaction between silicene and the substrate.

On the other hand, stacking has been demonstrated to be an effective tool for band gap opening in the case of graphene.[40] We therefore investigate three $MgBr_2(0001)$−silicene−$MgBr_2(0001)$ sandwiches, namely, configurations AC, BC, and CC, where the two letters refer to the configurations of the two interfaces. The three configurations are energetically almost degenerate with a maximal difference of 5 meV per atom. Configuration CC is favorable with a binding energy of 127 meV per Si atom. The band gap turns out to be 31 meV, which is larger than that in configuration C (13 meV), and the Dirac point is located 9 meV above the Fermi level. Because compressive strain increases the band gap of silicene, as shown for $MgCl_2$, we study biaxial strain ranging from −2% (compressive) to 2% (tensile) for $MgBr_2(0001)$−silicene−$MgBr_2(0001)$ sandwiches, as illustrated in Figure 7. The band gap decreases with compressive strain because of the reduced buckling.[36] The calculated values of 33 and 28 meV for −2% and 2% strain are about 6% larger and 8% smaller than those in the unstrained case. The lower branch of the Dirac cone is located 0−8 meV below the Fermi level and the upper branch 22−28 meV above it (Dirac point 7−14 meV above the Fermi level). Figure 8 shows charge density differences for configuration CC under strain. The charge redistribution in the interstitial regions of the sandwiches decreases from compression to tension because of the reduced interaction between silicene and the substrate.

4. CONCLUSIONS

The structural and electronic properties of silicene on $MgX_2(0001)$ (X = Cl, Br, and I) substrates have been investigated by first-principles calculations. Lateral shifts between silicene and the substrate modify the total energy only slightly, reflecting weak van der Waals interactions. Still, the charge redistribution at the interface depends critically on such shifts. All of the substrates are predicted to well preserve the Dirac cone of silicene with minor p doping. Application of an external electric field and stacking have been suggested to increase the band gap of silicene beyond the thermal energy at room temperature. The proposed substrates hardly perturb the silicene states because of a lack of dangling bonds.

AUTHOR INFORMATION

Corresponding Author

*E-mail: Udo.Schwingenschlogl@kaust.edu.sa.

Notes

The authors declare no competing financial interest.

ACKNOWLEDGMENTS

Research reported in this publication was supported by the King Abdullah University of Science and Technology (KAUST).

REFERENCES

(1) Novoselov, K. S.; Geim, A. K.; Morozov, S. V.; Jiang, D.; Zhang, Y.; Dubonos, S. V.; Grigorieva, I. V.; Firsov, A. A. Electric Field Effect in Atomically Thin Carbon Films. *Science* **2004**, *306*, 666−669.

(2) Castro Neto, A. H.; Guinea, F.; Peres, N. M. R.; Novoselov, K. S.; Geim, A. K. The Electronic Properties of Graphene. *Rev. Mod. Phys.* **2009**, *81*, 109−162.

(3) Novoselov, K. S.; Fal'ko, V. I.; Colombo, L.; Gellert, P. R.; Schwab, M. G.; Kim, K. A Roadmap for Graphene. *Nature* **2012**, *490*, 192−200.

(4) Takeda, K.; Shiraishi, K. Theoretical Possibility of Stage Corrugation in Si and Ge Analogs of Graphite. *Phys. Rev. B* **1994**, *50*, 14916−14922.

(5) Cahangirov, S.; Topsakal, M.; Aktürk, E.; Sahin, H.; Ciraci, S. Two- and One-Dimensional Honeycomb Structures of Silicon and Germanium. *Phys. Rev. Lett.* **2009**, *102*, 236804.

(6) Liu, C.; Feng, W.; Yao, Y. Quantum Spin Hall Effect in Silicene and Two-Dimensional Germanium. *Phys. Rev. Lett.* **2011**, *107*, 076802.
(7) Fleurence, A.; Friedlein, R.; Ozaki, T.; Kawai, H.; Wang, Y.; Yamada-Takamura, Y. Experimental Evidence for Epitaxial Silicene on Diboride Thin Films. *Phys. Rev. Lett.* **2012**, *108*, 245501.
(8) Meng, L.; Wang, Y.; Zhang, L.; Du, S.; Wu, R.; Li, L.; Zhang, Y.; Li, G.; Zhou, H.; Hofer, W. A.; Gao, H. Buckled Silicene Formation on Ir(111). *Nano Lett.* **2013**, *13*, 685−690.
(9) Vogt, P.; De Padova, P.; Quaresima, C.; Avila, J.; Frantzeskakis, E.; Asensio, M. C.; Resta, A.; Ealet, B.; Le Lay, G. Silicene: Compelling Experimental Evidence for Graphenelike Two-Dimensional Silicon. *Phys. Rev. Lett.* **2012**, *108*, 155501.
(10) Tsoutsou, D.; Xenogiannopoulou, E.; Golias, E.; Tsipas, P.; Dimoulas, A. Evidence for Hybrid Surface Metallic Band in (4 × 4) Silicene on Ag(111). *Appl. Phys. Lett.* **2013**, *103*, 231604.
(11) Kaltsas, D.; Tsetseris, L.; Dimoulas, A. Structural Evolution of Single-layer Films during Deposition of Silicon on Silver: A First-principles Study. *J. Phys.: Condens. Matter* **2012**, *24*, 442001.
(12) Wang, Y.; Cheng, H. Absence of a Dirac Cone in Silicene on Ag(111): First-principles Density Functional Calculations with a Modified Effective Band Structure Technique. *Phys. Rev. B* **2013**, *87*, 245430.
(13) Lin, C.-L.; Arafune, R.; Kawahara, K.; Kanno, M.; Tsukahara, N.; Minamitani, E.; Kim, Y.; Kawai, M.; Takagi, N. Substrate-Induced Symmetry Breaking in Silicene. *Phys. Rev. Lett.* **2013**, *110*, 076801.
(14) Ding, Y.; Wang, Y. Electronic Structures of Silicene/GaS Heterosheets. *Appl. Phys. Lett.* **2013**, *103*, 043114.
(15) Houssa, M.; van den Broek, B.; Scalise, E.; Pourtois, G.; Afanas'ev, V. V.; Stesmans, A. An Electric Field Tunable Energy Band Gap at Silicene/(0001) ZnS Interfaces. *Phys. Chem. Chem. Phys.* **2013**, *15*, 3702−3705.
(16) Bhattacharya, A.; Bhattacharya, S.; Das, G. P. Exploring Semiconductor Substrates for Silicene Epitaxy. *Appl. Phys. Lett.* **2013**, *103*, 123113.
(17) Mattausch, A.; Pankratov, O. *Ab Initio* Study of Graphene on SiC. *Phys. Rev. Lett.* **2007**, *99*, 076802.
(18) Ramasubramaniam, A.; Medhekar, N. V.; Shenoy, V. B. Substrate-induced Magnetism in Epitaxial Graphene Buffer Layers. *Nanotechnology* **2009**, *20*, 275705.
(19) Liu, H.; Gao, J.; Zhao, J. Silicene on Substrates: A Way to Preserve or Tune Its Electronic Properties. *J. Phys. Chem. C* **2013**, *117*, 10353−10359.
(20) Kokott, S.; Pflugradt, P.; Matthes, L.; Bechstedt, F. Nonmetallic Substrates for Growth of Silicene: An *Ab Initio* Prediction. *J. Phys.: Condens. Matter* **2014**, *26*, 185002.
(21) Varchon, F.; Feng, R.; Hass, J.; Li, X.; Nguyen, B. N.; Naud, C.; Mallet, P.; Veuillen, J.-Y.; Berger, C.; Conrad, E. H.; Magaud, L. Electronic Structure of Epitaxial Graphene Layers on SiC: Effect of the Substrate. *Phys. Rev. Lett.* **2007**, *99*, 126805.
(22) Poon, S. W.; Chen, W.; Wee, A. T. S.; Tok, E. S. Growth Dynamics and Kinetics of Monolayer and Multilayer Graphene on a 6H-SiC(0001) Substrate. *Phys. Chem. Chem. Phys.* **2010**, *12*, 13522−13533.
(23) Liu, Y.; Shu, H.; Liang, P.; Cao, D.; Chen, X.; Lu, W. Structural, Electronic, and Optical Properties of Hydrogenated Few-layer Silicene: Size and Stacking Effects. *J. Appl. Phys.* **2013**, *114*, 094308.
(24) Gao, N.; Li, J.; Jiang, Q. Bandgap Opening in Silicene: Effect of Substrates. *Chem. Phys. Lett.* **2014**, *592*, 222−226.
(25) Fairbrother, D. H.; Roberts, J. G.; Rizzi, S.; Somorjai, G. A. Structure of Monolayer and Multilayer Magnesium Chloride Films Grown on Pd(111). *Langmuir* **1997**, *13*, 2090−2096.
(26) Fairbrother, D.; Roberts, J. G.; Somorjai, G. A. The Growth of Magnesium Chloride Monolayer and Multilayer Structures on Different Transition Metal (Pt, Pd, Rh) Single Crystals with Varied Orientations. *Surf. Sci.* **1998**, *399*, 109−122.
(27) Kresse, G.; Furthmüller, J. Efficient Iterative Schemes for Ab Initio Total-energy Calculations Using a Plane-wave Basis Set. *Phys. Rev. B* **1996**, *54*, 11169−11186.
(28) Kresse, G.; Joubert, D. From Ultrasoft Pseudopotentials to the Projector Augmented-wave Method. *Phys. Rev. B* **1999**, *59*, 1758−1775.
(29) Perdew, J. P.; Burke, K.; Ernzerhof, M. Generalized Gradient Approximation Made Simple. *Phys. Rev. Lett.* **1996**, *77*, 3865−3868.
(30) Grimme, S. Semiempirical GGA-type Density Functional Constructed with a Long-range Dispersion Correction. *J. Comput. Chem.* **2006**, *27*, 1787−1799.
(31) Togo, A.; Oba, F.; Tanaka, I. First-principles Calculations of the Ferroelastic Transition between Rutile-type and $CaCl_2$-type SiO_2 at High Pressures. *Phys. Rev. B* **2008**, *78*, 134106.
(32) Parlinski, K.; Li, Z. Q.; Kawazoe, Y. First-Principles Determination of the Soft Mode in Cubic ZrO_2. *Phys. Rev. Lett.* **1997**, *78*, 4063−4066.
(33) Harrison, N. M.; Saunders, V. R. The Structural Properties of β-$MgCl_2$; An *Ab Initio* Study. *J. Phys.: Condens. Matter* **1992**, *4*, 3873.
(34) Pies, W.; Weiss, A. In Key Elements: F, Cl, Br, I. *Landolt-Börnstein - Group III Condensed Matter*; Hellwege, K.-H., Hellwege, A., Eds.; Springer: Berlin, 1973; Vol. *7a*; pp 520−529.
(35) Brogan, M. A.; Blake, A. J.; Wilson, C.; Gregory, D. H. Magnesium Diiodide, MgI_2. *Acta Crystallogr., Sect. C: Cryst. Struct. Commun.* **2003**, *59*, i136−i138.
(36) Huang, S.; Kang, W.; Yang, L. Electronic Structure and Quasiparticle Bandgap of Silicene Structures. *Appl. Phys. Lett.* **2013**, *102*, 133106.
(37) Sadeghi, H. Electrical Transport Model of Silicene as a Channel of Field Effect Transistor. *J. Nanosci. Nanotechnol.* **2014**, *14*, 4178−4184.
(38) Ni, Z.; Liu, Q.; Tang, K.; Zheng, J.; Zhou, J.; Qin, R.; Gao, Z.; Yu, D.; Lu, J. Tunable Bandgap in Silicene and Germanene. *Nano Lett.* **2012**, *12*, 113−118.
(39) Drummond, N. D.; Zólyomi, V.; Fal'ko, V. I. Electrically Tunable Band Gap in Silicene. *Phys. Rev. B* **2012**, *85*, 075423.
(40) Quhe, R.; Zheng, J.; Luo, G.; Liu, Q.; Qin, R.; Zhou, J.; Yu, D.; Nagase, S.; Mei, W.-N.; Gao, Z.; Lu, J. Tunable and Sizable Band Gap of Single-layer Graphene Sandwiched between Hexagonal Boron Nitride. *NPG Asia Mater.* **2012**, *4*, e6.